NASr-65(18)

Report No. IITRI-V6032-8

COMPOSITIONAL ANALYSIS OF LUNAR AND PLANETARY SURFACES USING NEUTRON CAPTURE GAMMA RAYS

for

Dr. V. R. Wilmarth
National Aeronautics and Space Administration
Washington, D. C. 20546

Report No. IITRI-V6032-8

COMPOSITIONAL ANALYSIS OF LUNAR AND PLANETARY SURFACES USING NEUTRON CAPTURE GAMMA RAYS

January 1, 1968, to March 31, 1968

Prepared by

J. W. Mandler

R. A. Semmler

Submitted by

IIT RESEARCH INSTITUTE
Technology Center
10 West 35th Street
Chicago, Illinois 60616

for

Dr. V. R. Wilmarth
National Aeronautics and Space Administration
Washington, D. C. 20546

April 1968

FOREWORD

This is Report No. IITRI-V6032-8 (formerly A6155) under Contract No. NASr 65(18), entitled "Compositional Analysis of Lunar and Planetary Surfaces Using Neutron Capture Gamma Rays," covering the period January 1, 1968, to March 31, 1968.

The following personnel have contributed to the work described in this report: J. H. Reed, principal investigator, J. W. Mandler, co-investigator, R. A. Semmler, and R. S. Ryskiewicz.

Respectfully submitted
IIT RESEARCH INSTITUTE

J. W. Mandler
Associate Physicist

J. H. Reed
Research Physicist-Group Leader
Nuclear and Radiation Physics

Approved by:

R. B. Moler
Manager
Nuclear and Radiation Physics

/gjw

ABSTRACT

The detection and quantitative determination of the presence of hydrogen is of prime concern to the capture gamma-ray experiment. The use of the hydrogenous neutron reflector has interfered with this measurement, due to the detection of hydrogen capture gamma rays produced in the reflector. During this reporting period, a study was begun to determine how the detection of hydrogen could be accomplished without forfeiting the use of a neutron reflector. Results indicate that this can be done successfully if the crystal is shielded from the gamma rays produced in the neutron reflector.

IIT Research Institute has been assigned the task of designing and fabricating the detector probe that will be used in the formal demonstration of the combined neutron experiment. To accomplish this task, it is necessary to select a suitable material and shape for the fast neutron shield, to determine the neutron reflector thickness necessary to obtain good quality capture gamma-ray spectra, to determine the effect of a neutron reflector on the inelastic spectrum, and to decide whether shielding will be necessary to eliminate electromagnetic interferences.

On the basis of cross section and other considerations molybdenum was chosen as a good compromise material for the fast neutron shadow shield. Experiments indicate that the capture, inelastic, and cyclic activation spectra are essentially independent of the shadow shield material if reasonable materials are used. Experimental data also indicate that the neutron reflector has no apparent effect on the inelastic spectrum. The thickness of the neutron reflector to be used has not yet been determined. While more experimentation with different samples will be necessary before the thickness decision can

Major impact upon total probe weight

be made, it would appear that a thickness between 4 and 8 cm will be necessary. The basic geometry of the probe has therefore been designed to accommodate both a 4-cm- and an 8-cm-thick neutron reflector. The shape of the shadow shield was designed to shield the crystal from fast neutrons and from gamma rays originating in the reflector and in the neutron generator itself.

Experiments also indicate that the placement of electromagnetic shielding material around the neutron generator, photomultiplier tube, and preamplifier will be necessary to eliminate electromagnetic interferences produced by the voltage multiplier in the generator.

TABLE OF CONTENTS

LIST OF FIGURES

LIST OF FIGURES (Continued)

LIST OF TABLES

I. DETECTION OF HYDROGEN

The use of a hydrogenous neutron reflector has been shown to interfere with the detection of hydrogen in the sample. Since this interference is a serious concern, a study was begun during this reporting period to determine how the detection of hydrogen using capture gamma rays can be accomplished without forfeiting the use of a neutron reflector.

Figure 1 shows the capture gamma-ray spectrum from basalt obtained during the sampling period 20 to 254 μsec after the neutron burst. The pulse rate was 530 pps, the neutron output was 4150 ± 540 neutrons per pulse,* and a 4-cm-thick polyethylene reflector was located above the target. Figure 2 shows the capture gamma-ray spectrum from basalt obtained under the same conditions as for Figure 1 with the exceptions that the neutron output was 4740 ± 610 neutrons per pulse and that no reflector was used.

In Figure 2 the 2.22-MeV H(n,γ) peak is due solely to hydrogen in the basalt sample, since no reflector was used. A comparison (after normalization to a common thermal neutron flux by means of the number of counts in the 7.6-MeV Fe(n,γ) peaks) of the 2.22-MeV H(n,γ) peaks in Figures 1 and 2 indicates that approximately 50 percent of the counts in the H(n,γ) peak in Figure 1 are due to the reflector, the remainder coming from the basalt sample.

Figure 3 shows the capture gamma-ray spectrum from basalt obtained under the same conditions as for Figure 1 with the exceptions that the neutron output was 3920 ± 520 neutrons per pulse and that a 4-in.-thick lead shield was located between the crystal and the polyethylene neutron reflector. The purpose of the lead shield was to prevent hydrogen capture gamma rays originating in the reflector from reaching the crystal (4-in. of

*See Appendix A for a description of the present neutron monitoring system.

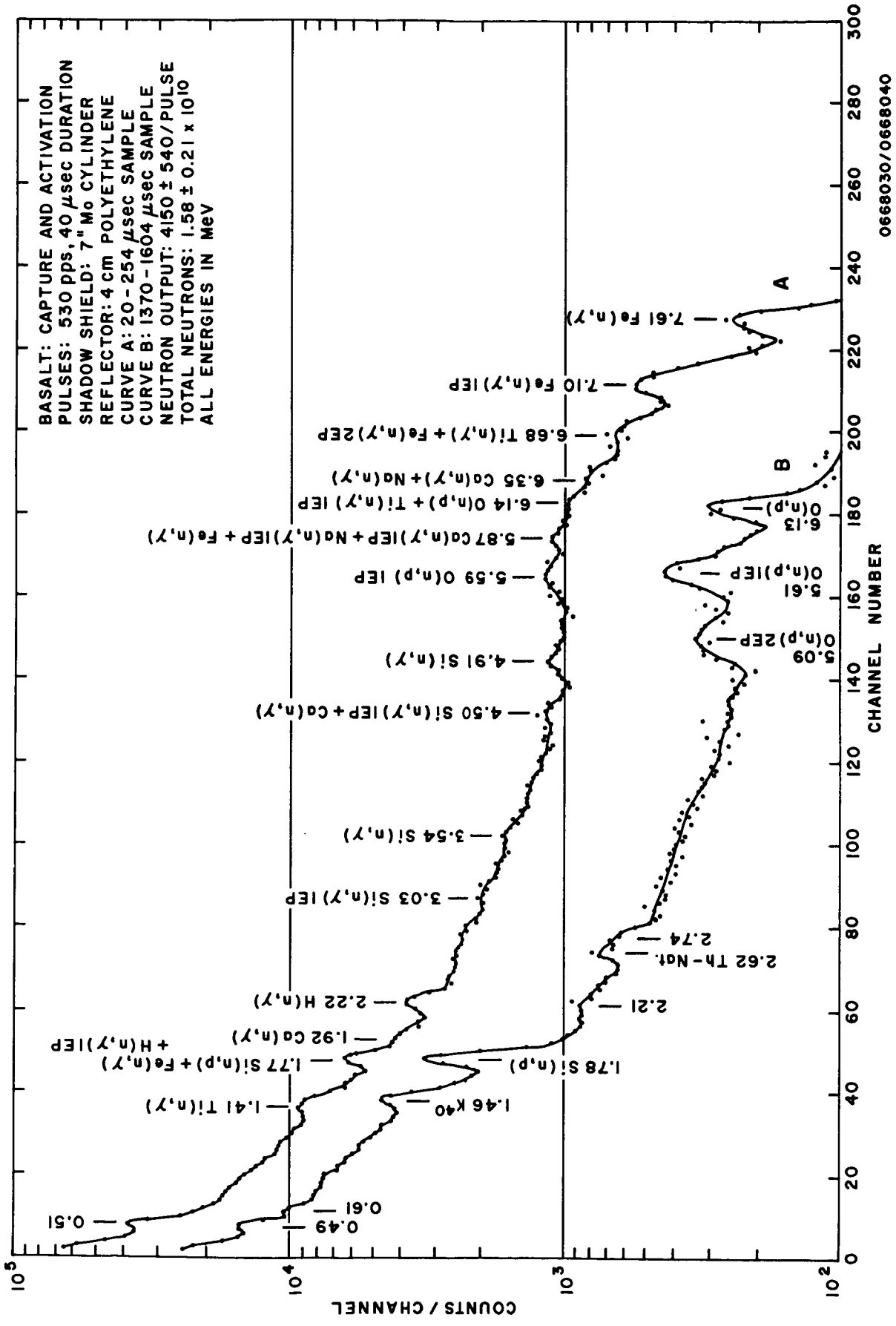

Figure 1 CAPTURE AND CYCLIC ACTIVATION SPECTRA OF BASALT (4-cm-thick Polyethylene Reflector, 7 in. Mo Shadow Shield)

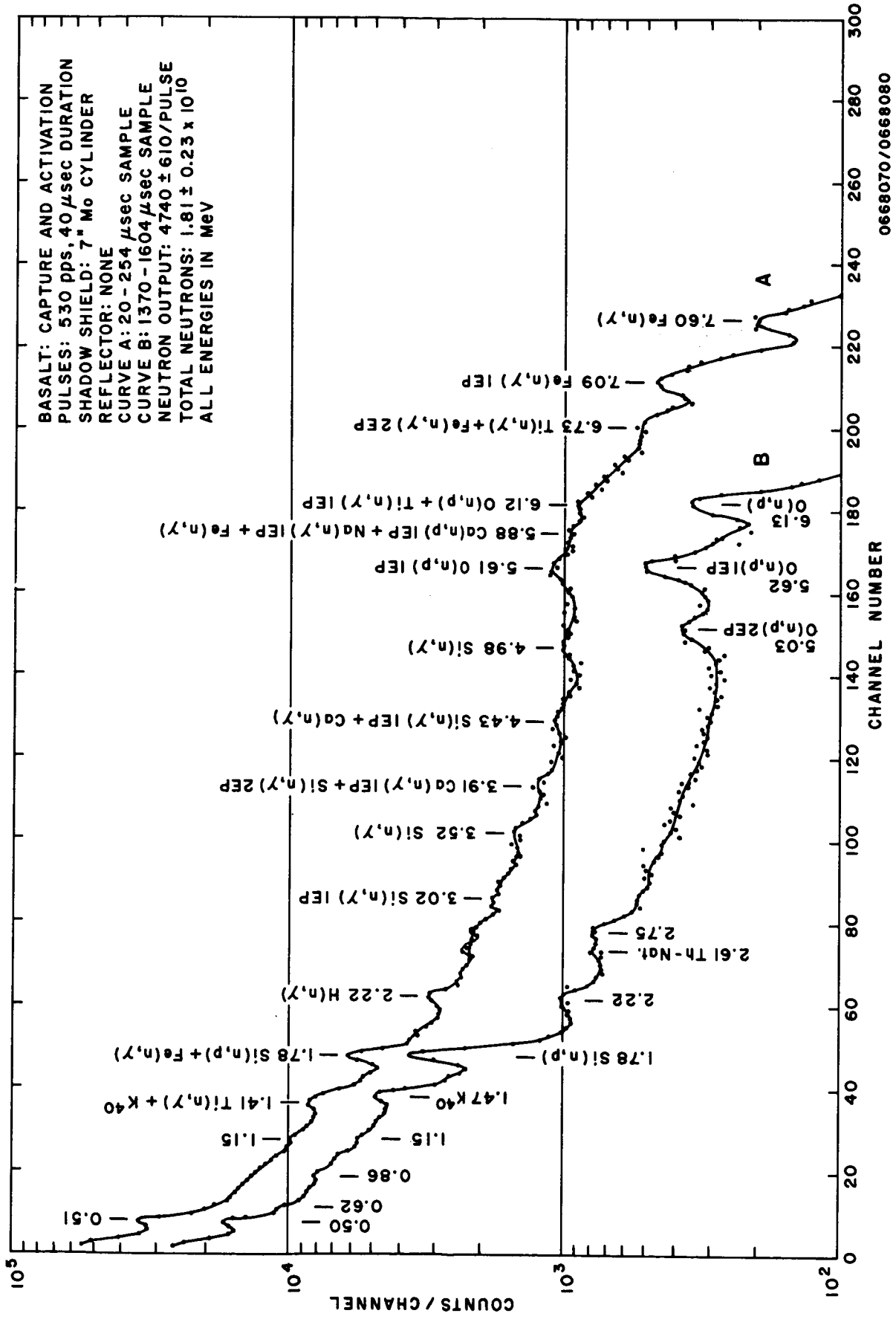

Figure 2 CAPTURE AND CYCLIC ACTIVATION SPECTRA OF BASALT (No Reflector, 7 in. Mo Shadow Shield)

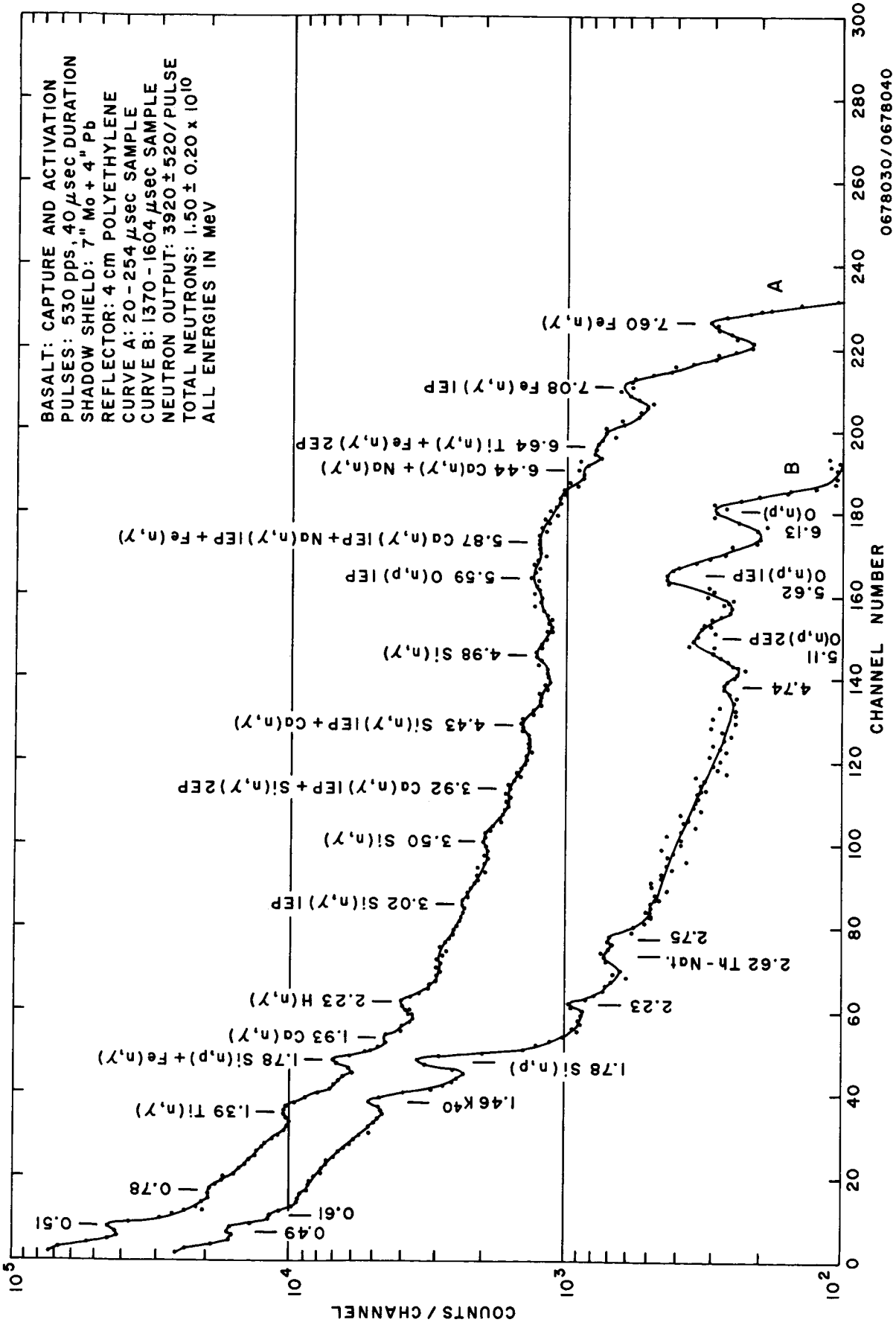

Figure 3 CAPTURE AND CYCLIC ACTIVATION SPECTRA OF BASALT (4-cm-thick Polyethylene Reflector, 7 in. Mo + 4 in. Pb Shadow Shield)

lead attenuates the 2.22-MeV hydrogen capture gamma rays by about a factor of 200). In Figure 3, the number of counts in the 2.22-MeV H(n,γ) peak has indeed been reduced to about the number occurring in the spectrum obtained using no neutron reflector (Figure 2).

The results of the above measurements indicate that the detection of hydrogen can be accomplished using capture gamma rays without forfeiting the use of a neutron reflector if the crystal is shielded from the gamma rays produced in the reflector. Aside from the beneficial effect of eliminating the counts due to gamma rays produced in the reflector, this shield appears to have no effect on the capture gamma-ray spectrum.

II. DEVELOPMENT OF A PROBE

IIT Research Institute has been assigned the task of designing and fabricating the probe to be used with the neutron generator built by the SANDIA Corp. To accomplish this task, decisions had to be made concerning various experimental parameters. These included choosing a suitable material and shape for the fast-neutron shadow shield, selecting the thickness of the Li^6 thermal neutron shield, determining the reflector thickness necessary to obtain good capture gamma-ray spectra, and determining whether shielding would be necessary to eliminate electromagnetic interference.

Selection of the Fast-Neutron Shadow Shield Material

The first screening of possible shield materials was based on the fast-neutron-removal cross section which is approximately independent of energy over the range of 0.1 to 14 MeV. Figure 4 shows the macroscopic-removal cross section (Σ_r) as a function of atomic number for all elements. Figure 5 shows the same data after dividing by the density to convert to a mass absorption coefficient (μ_r). For a minimum length shield, the value Σ_r should be large. For a minimum weight shield, the value of μ_r should be large.

As a compromise between weight and length considerations, materials were selected with a large value for the product $\mu_r\Sigma_r$. Contour lines are drawn on Figure 4 for fixed values of $\mu_r\Sigma_r = 2 \times 10^{-3}$, 2.5×10^{-3}, and 3×10^{-3} to indicate the general trend of the $\mu_r\Sigma_r$ product. All materials above the value $\mu_r\Sigma_r = 2.3 \times 10^{-3}$ were retained for further evaluation. This cutoff value of $\mu_r\Sigma_r$ was chosen so that most of the common shielding materials would be included (lead, however, with $\mu\Sigma_r = 1.2 \times 10^{-3}$ is excluded). This initial list of elements is given in Table 1.

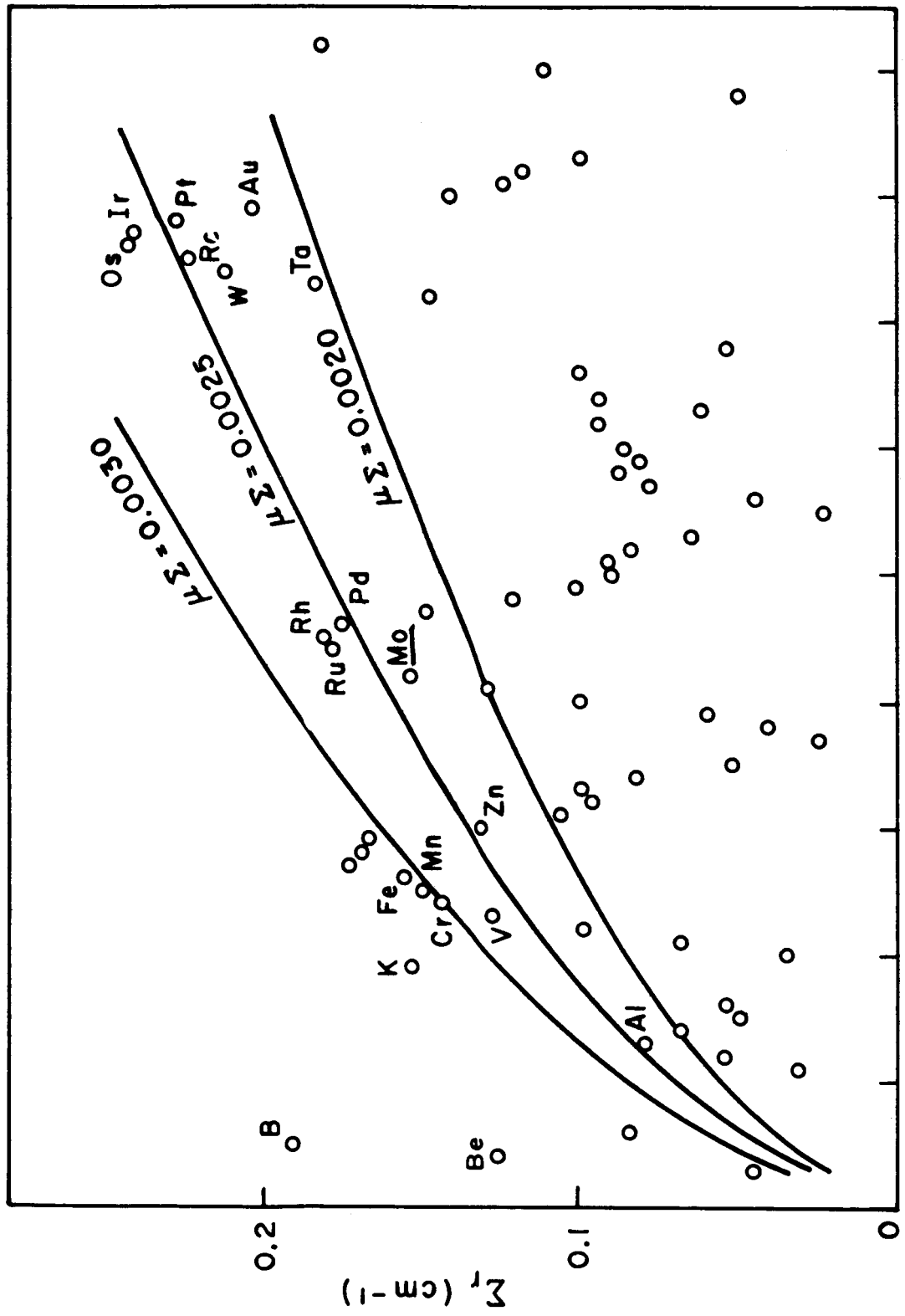

Figure 4 MACROSCOPIC-REMOVAL CROSS SECTION (Σ_r) AS A FUNCTION OF ATOMIC NUMBER

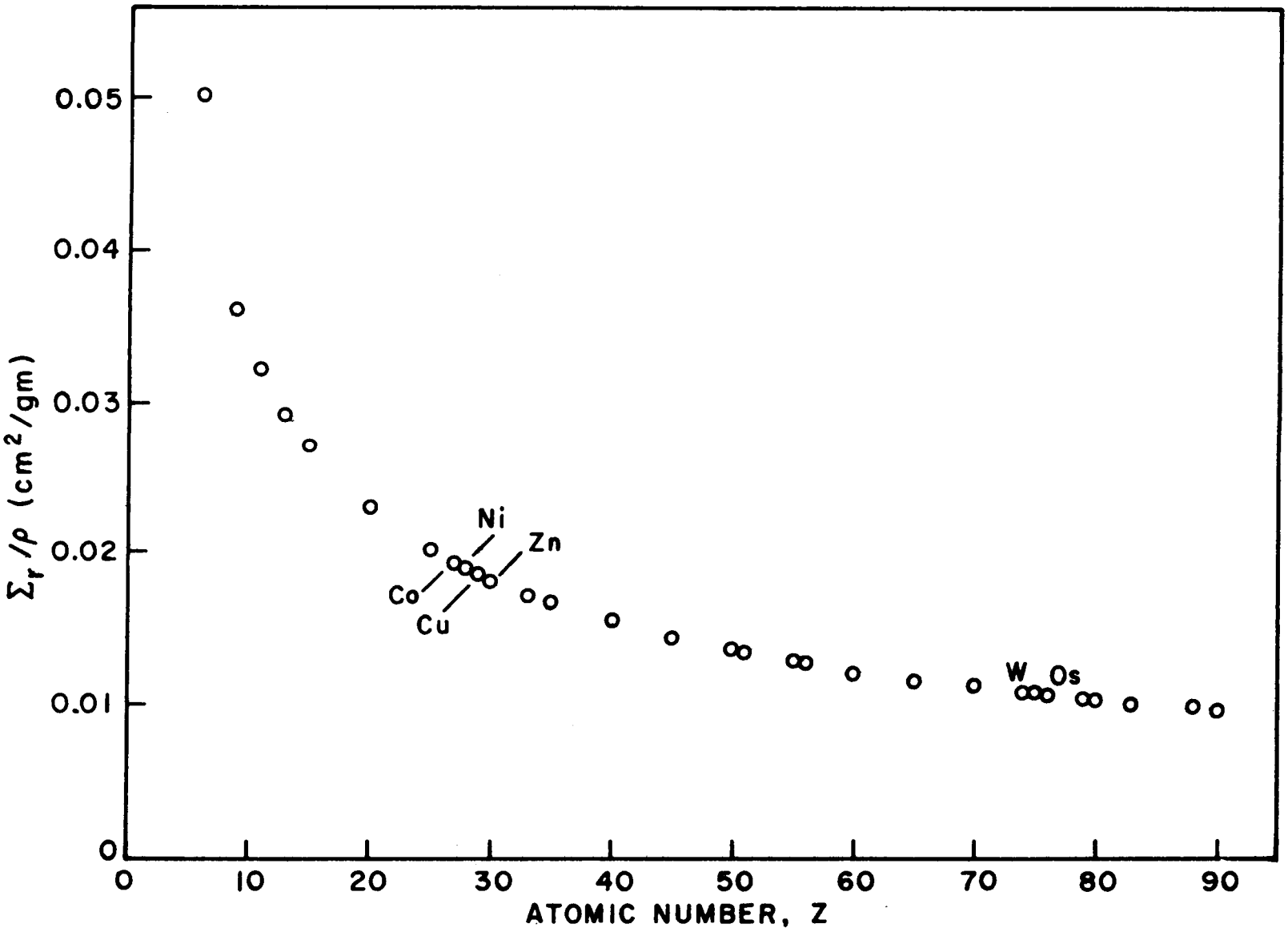

Figure 5 MASS ABSORPTION COEFFICIENT (μ_r) AS A FUNCTION OF ATOMIC NUMBER

Table 1 SELECTED INTERACTION RATES IN ELEMENTS WITH LARGE NEUTRON REMOVAL CROSS SECTIONS

Z	Element	$\mu_r \Sigma_r$ (10^{-3} cm/gm)	MOST SENSITIVE TO* Fast Activation (μg sensitivity)	Thermal Activation (μg sensitivity)	Σ_a (cm^{-1})	$\rho\mu_\gamma$ (10^{-2} cm^{-1})
5	Boron	11.0	[120]		[22.6]	[9.7]
4	Beryllium	8.4			(0.001)	[7.2]
6	Carbon	4.2	Excessive length (2X greater than Cu shield)			
3	Lithium	3.8	Excessive length (4X greater than Cu shield)			
19	Potassium	3.6	[580]		(0.03)	[3.8]
27	Cobalt	3.4		[5.5]	[3.23]	36.4
28	Nickel	3.2	(15,000)	(160,000)	0.41	38.1
29	Copper	3.1	[25.5]		0.32	37.4
26	Iron	3.1	Possible interference with sample			
25	Manganese	3.0	[400]	[35]	1.07	30.7
24	Chromium	3.0	[200]		0.25	29.0
23	Vanadium	2.7		[25]	0.35	24.4
45	Rhodium	2.6		[12.5]	[10.8]	51.6
76	Osmium	2.6		(7 x 10^5)	1.12	(98.4)
44	Ruthenium	2.6	(2,200)		(0.18)	50.0
77	Iridium	2.6		[3.35]	[30.9]	(98.3)
46	Palladium	2.5	(2,000)		0.55	50.4
75	Rhenium	2.4		(2,400)	[8.16]	(90.2)
78	Platinum	2.4	(5,400)	(1,600)	0.58	(95.3)
30	Zinc	2.4	(2,100)		(0.07)	30.1
74	Tungsten	2.3		[365]	1.19	(82.4)
42	Molybdenum	2.3	(4,000)		(0.17)	42.1
13	Aluminum	2.3	Possible interference with sample			

*Note that favorable values are enclosed in parentheses and unfavorable values are enclosed in brackets.

At this point, elements likely to be abundant in a lunar sample or which would require an excessively long shield were also excluded. These included iron, aluminum, lithium, and carbon. + Ni (?)

Four other characteristics were then examined for each of the elements remaining in Table 1. These were (1) fast-neutron activation, (2) thermal neutron activation, (3) thermal neutron capture gamma-ray production, and (4) gamma-ray absorption at 2 MeV.

The sensitivity to the first two interactions is indicated in Table 1 by published estimates of the minimum detectable mass when the interaction is used for elemental analysis. Values for the thermal neutron macroscopic absorption cross section (Σ_a) and gamma ray macroscopic cross section ($\rho\mu_\gamma$) are also given in Table 1. Favorable values (low Σ_a, high $\rho\mu_\gamma$) are enclosed in parentheses and poor values are in square brackets.

No one material was found to be ideal. A nickel shield has generally excellent characteristics except for a somewhat large capture gamma production rate. Ruthenium also looks good but is not generally available. Zinc and molybdenum also are attractive. However, other tabulations of elemental sensitivity using fast-neutron activation indicated a greater sensitivity for zinc than the tabulation reproduced here. Zinc was therefore excluded. (Tungsten was eliminated because it has a high thermal neutron activation cross section.) Molybdenum was finally chosen over nickel as a compromise material to avoid large rates for any of the interactions which could interfere with experimental measurements.

In order to determine the effect of the fast-neutron shadow shield on the observed spectra, capture, inelastic, and cyclic activation spectra were obtained from the large basalt sample using four different shadow shields: a 6 in.-long

truncated tungsten cone, a 6-in.-long truncated copper cone, a 7-in.-long copper cylinder, and a 7-in.-long molybdenum cylinder. Figures 6 through 9 show the capture and cyclic activation spectra obtained using the four shadow shields. The conditions (including source-to-crystal distance) under which these spectra were obtained were identical except for small differences in the neutron output. Figures 10 through 13 show the inelastic spectra obtained using the four shadow shields.

Figures 6 through 13 indicate that the spectral shapes of the capture, inelastic, and cyclic activation are not affected by the different shadow shields. However, the 0.51-MeV annihilation peak is smaller for tungsten or molybdenum shadow shields than it is when a copper shadow shield is used. They also show that the intensities of the peaks are greater for a truncated cone than for a cylindircal shadow shield. This is probably caused by the cylindrical shape shielding part of the sample between the target and the crystal from the neutrons, and thus moving the active volume farther from the crystal.

Reflector Thickness

In order to determine what reflector thickness is necessary to obtain good quality capture gamma-ray spectra, the iron capture gamma-ray peaks in Figures 1 (no reflector), 2 (4-cm-thick polyethylene reflector), and 9 (8-cm-thick polyethylene reflector) were analyzed. However, the large uncertainties due to the crude methods of analysis presently being used (no suitable computer program for data analysis is presently available) permit only a qualitative analysis. Qualitative results indicate that, although a reasonable capture gamma-ray spectrum can be obtained from basalt without a neutron reflector (Figure 1), the use of a reflector increases the intensities of the capture gamma-ray peaks and thus increases the quality of the spectrum.

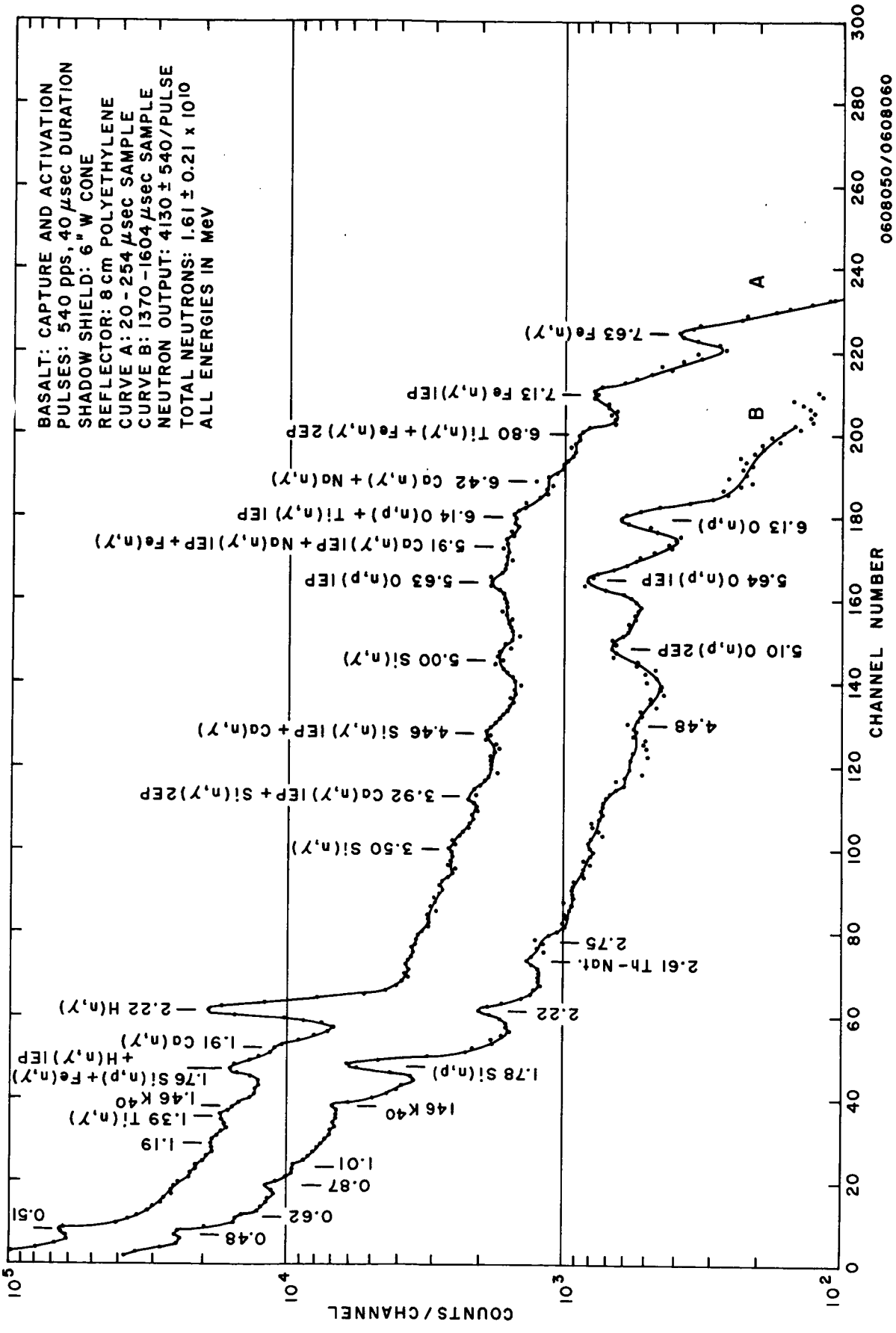

Figure 6 CAPTURE AND CYCLIC ACTIVATION SPECTRA OF BASALT (8-cm-thick Polyethylene Reflector, 6 in. W Shadow Shield)

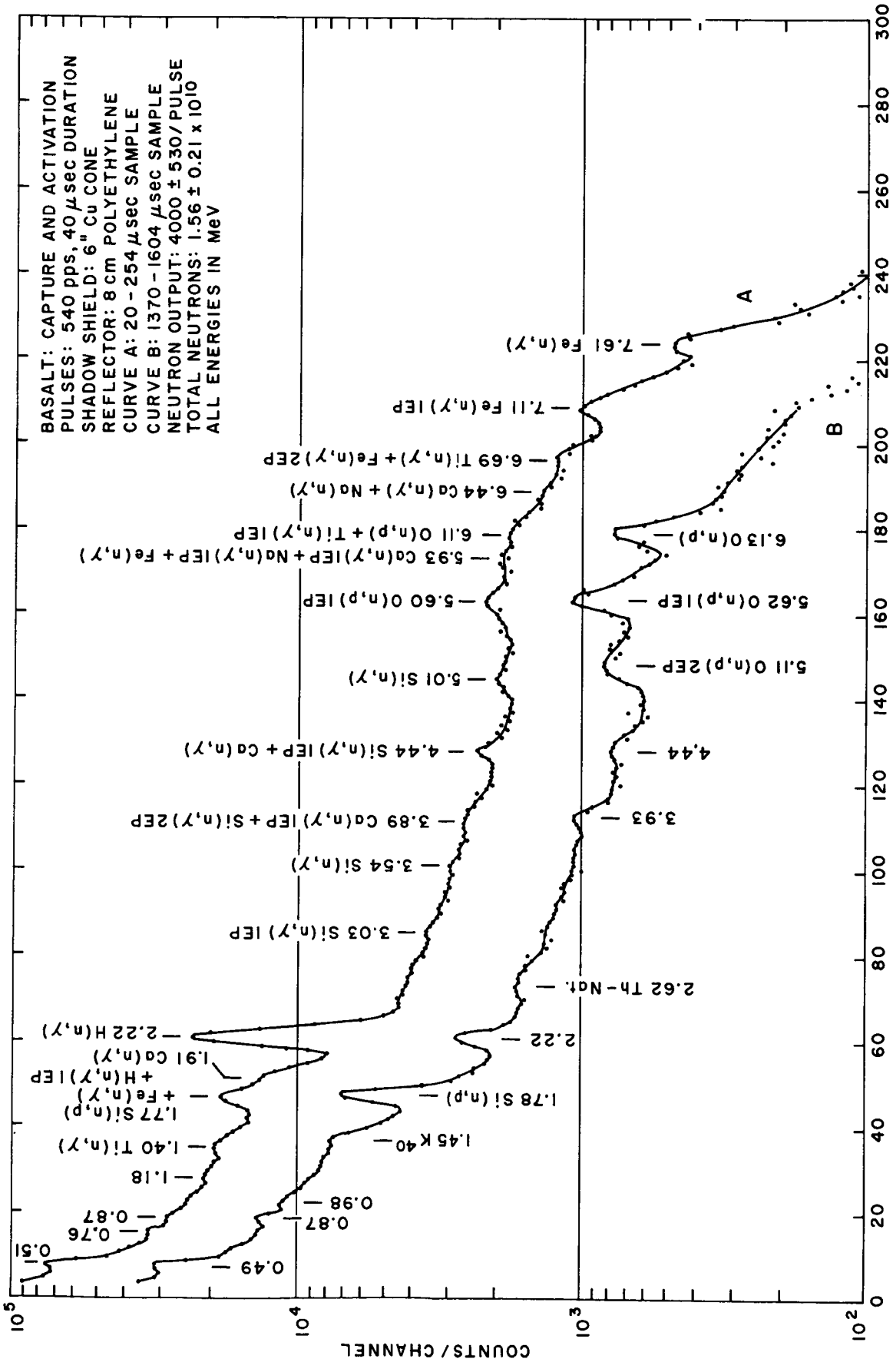

Figure 7 CAPTURE AND CYCLIC ACTIVATION SPECTRA OF BASALT (8-cm-thick Polyethylene Reflector, 6 in. Cu Shadow Shield)

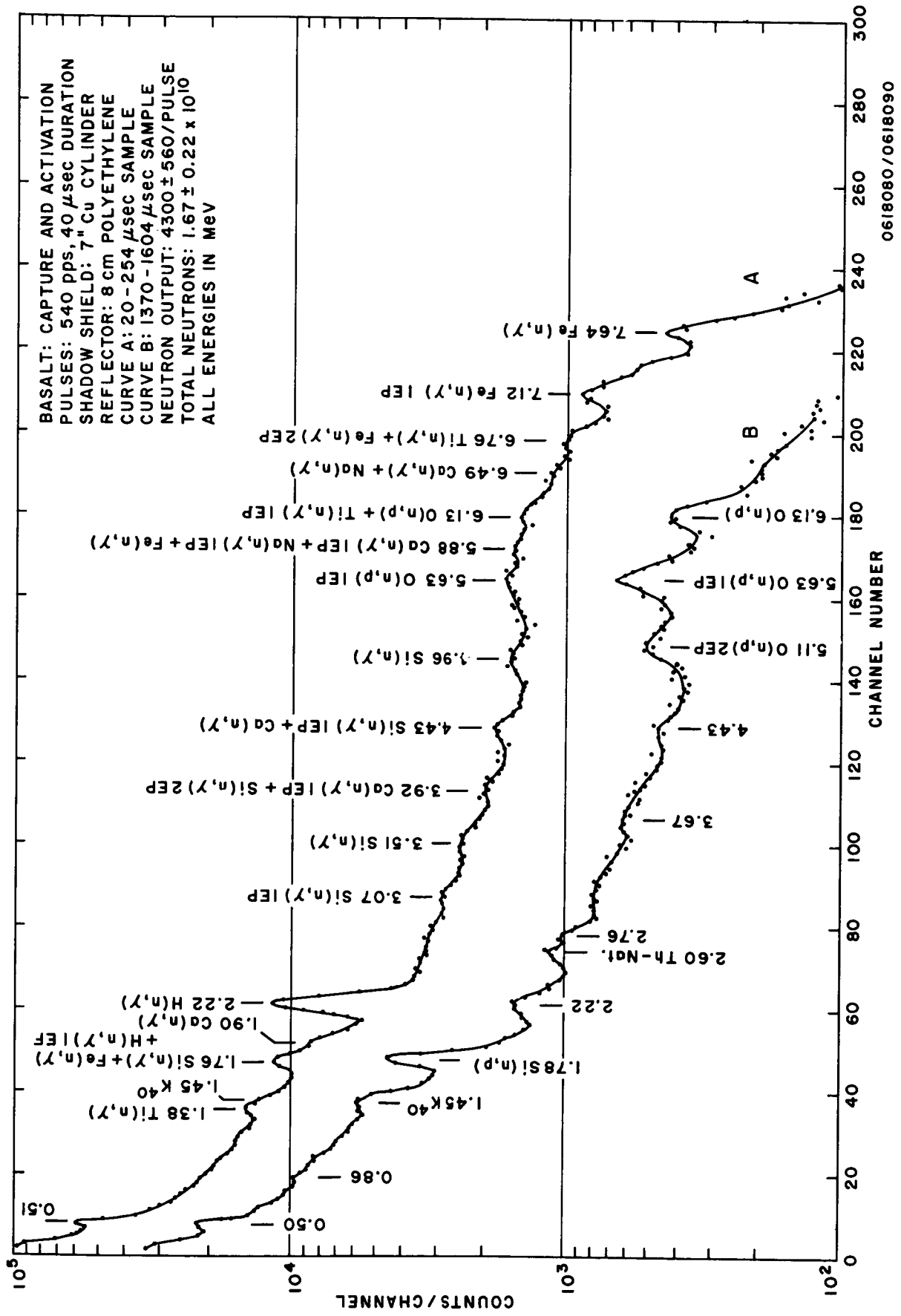

Figure 8 CAPTURE AND CYCLIC ACTIVATION SPECTRA OF BASALT (8-cm-thick Polyethylene Reflector, 7 in. Cu Shadow Shield)

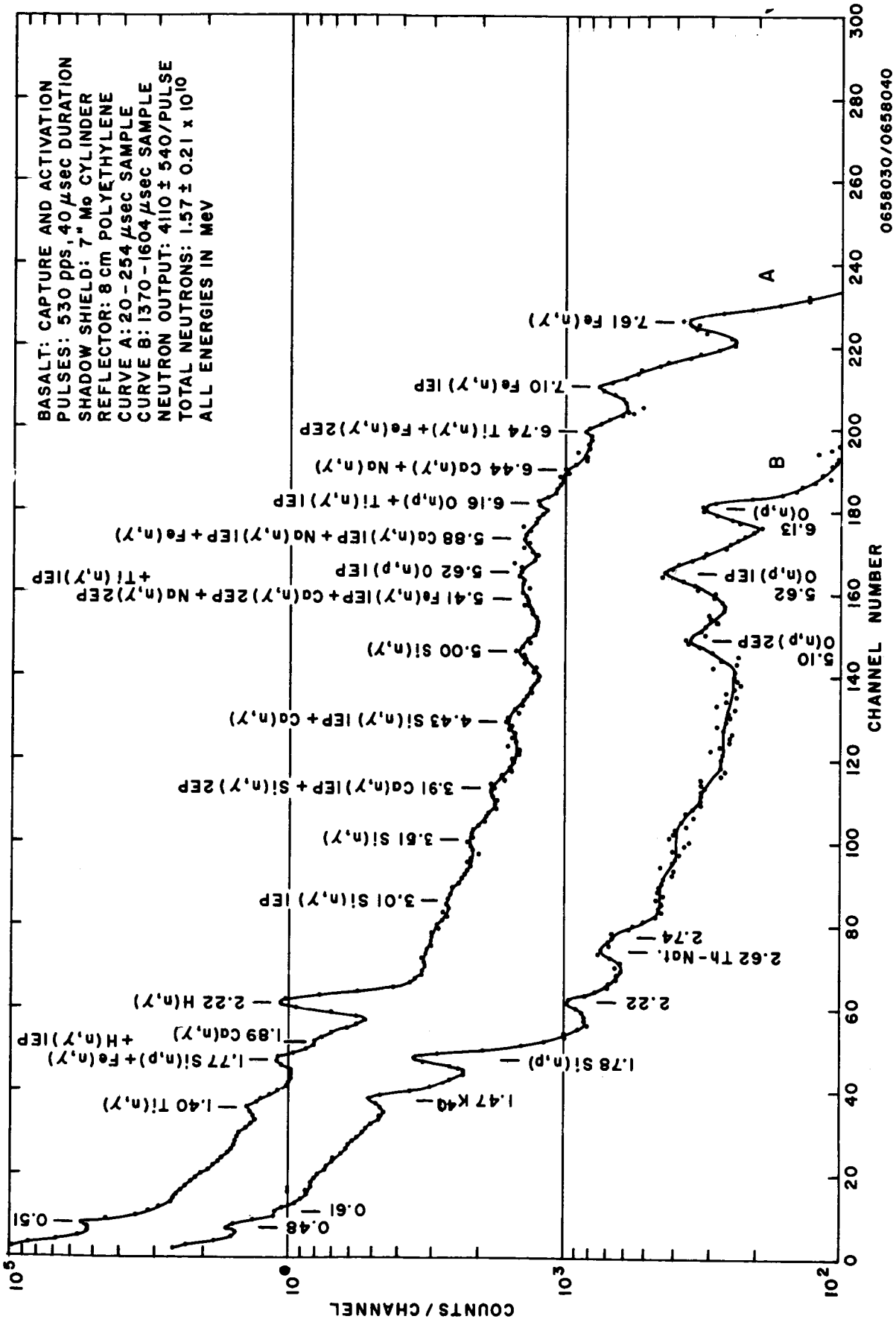

Figure 9 CAPTURE AND CYCLIC ACTIVATION SPECTRA OF BASALT (8-cm-thick Polyethylene Reflector, 7 in. Mo Shadow Shield)

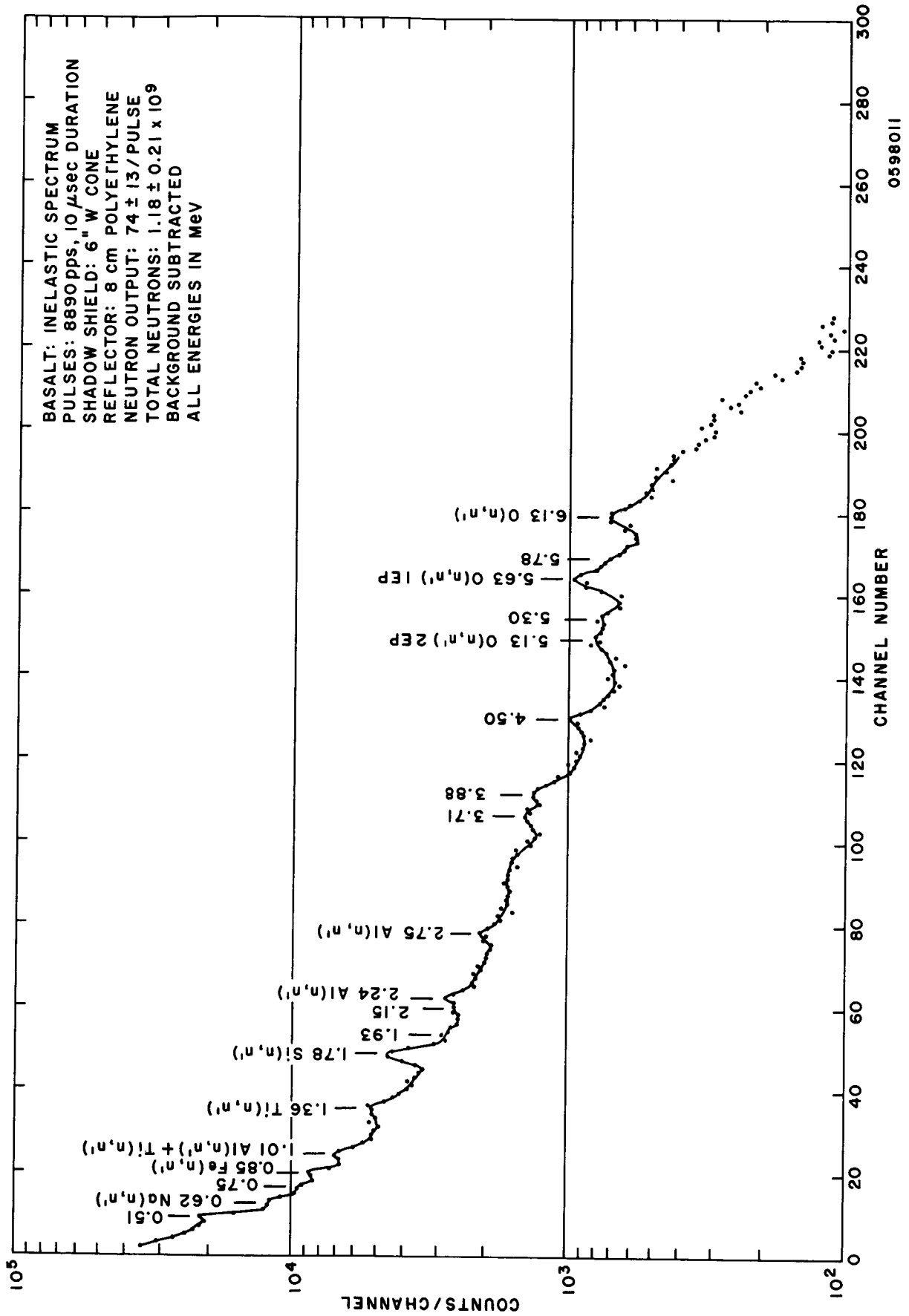

Figure 10 INELASTIC SPECTRUM OF BASALT (8-cm-thick Polyethylene Reflector, 6 in. W Shadow Shield)

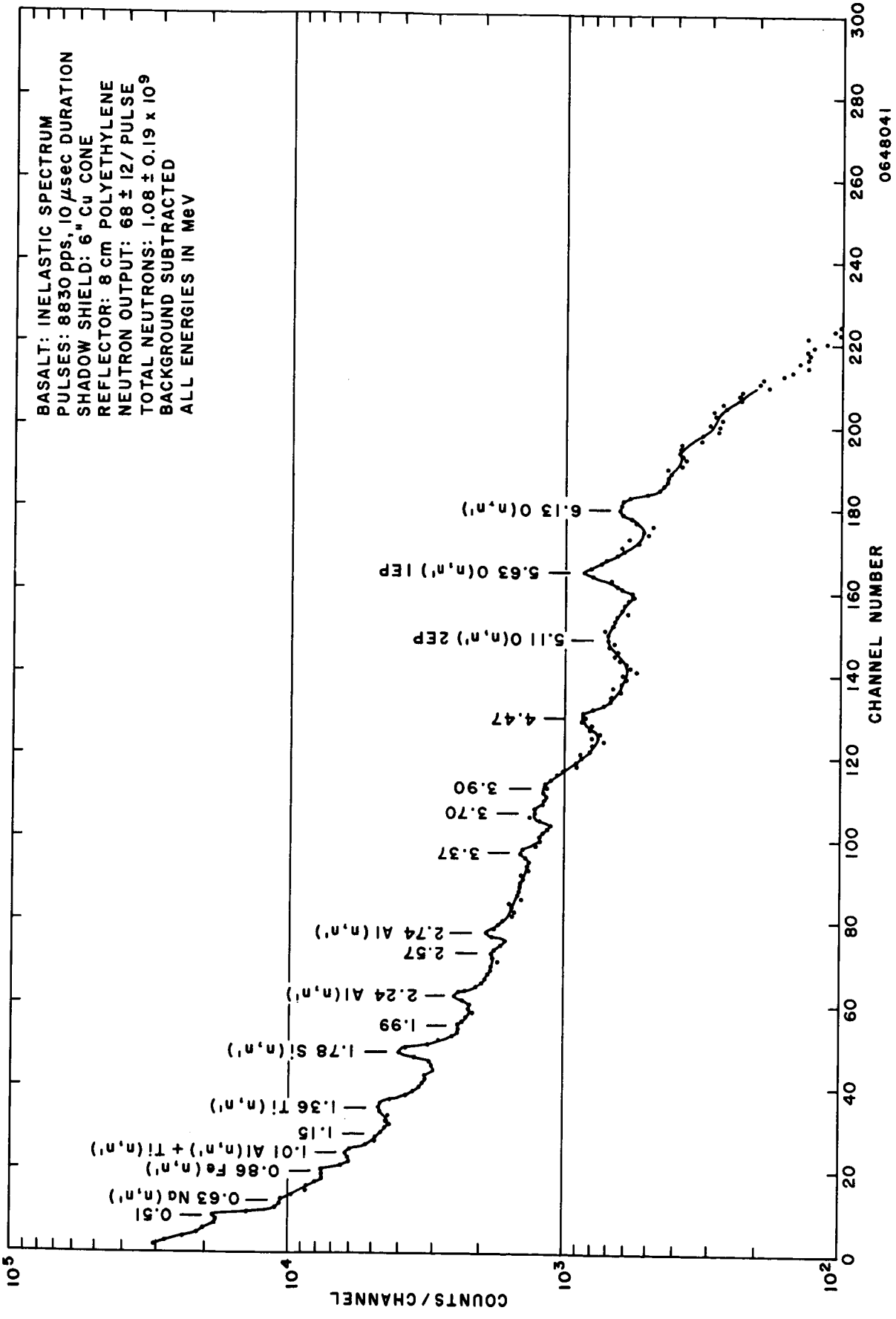

Figure 11 INELASTIC SPECTRUM OF BASALT (8-cm-thick Polyethylene Reflector, 6 in. Cu Shadow Shield)

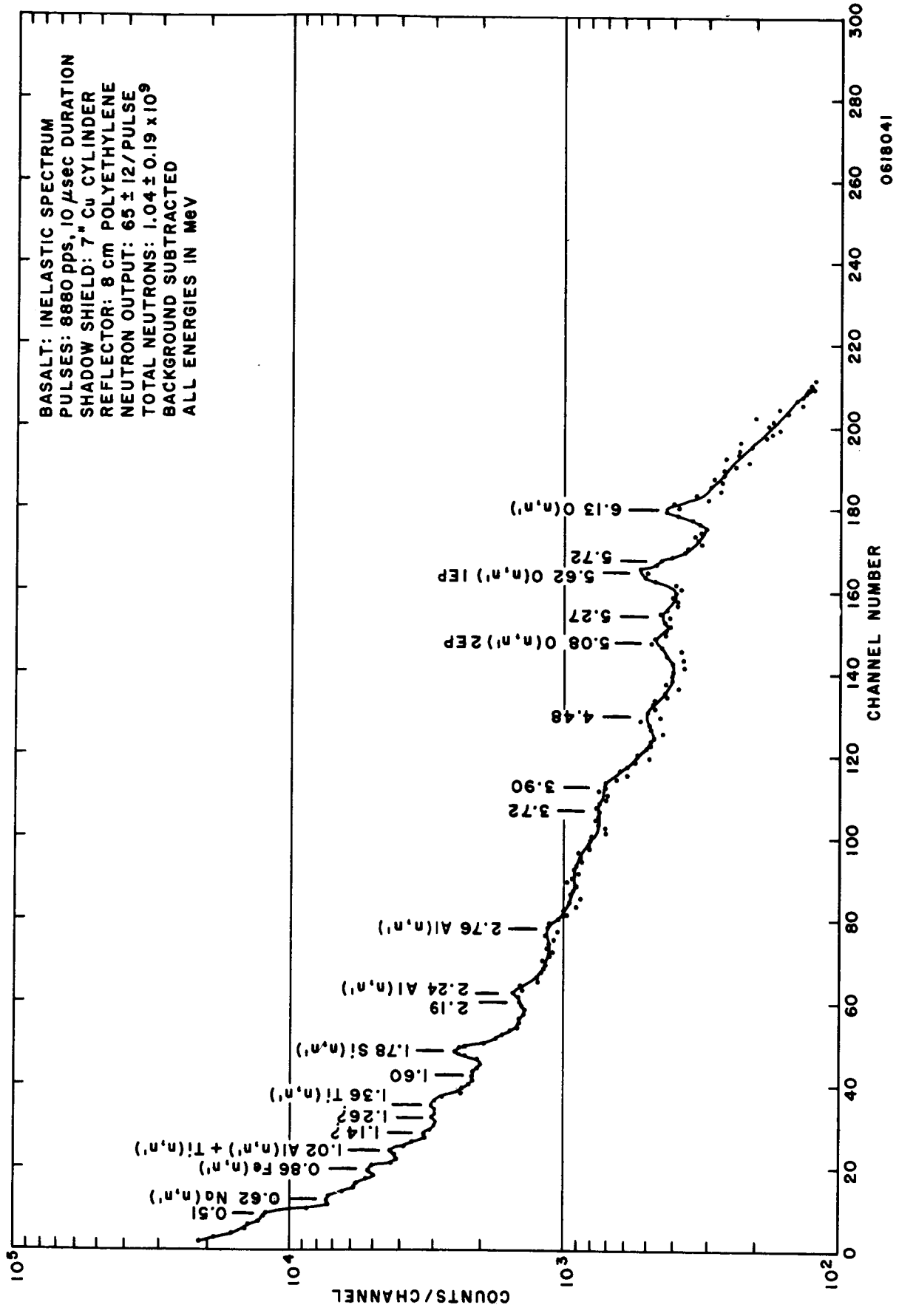

Figure 12 INELASTIC SPECTRUM OF BASALT (8-cm-thick Polyethylene Reflector, 7 in. Cu Shadow Shield)

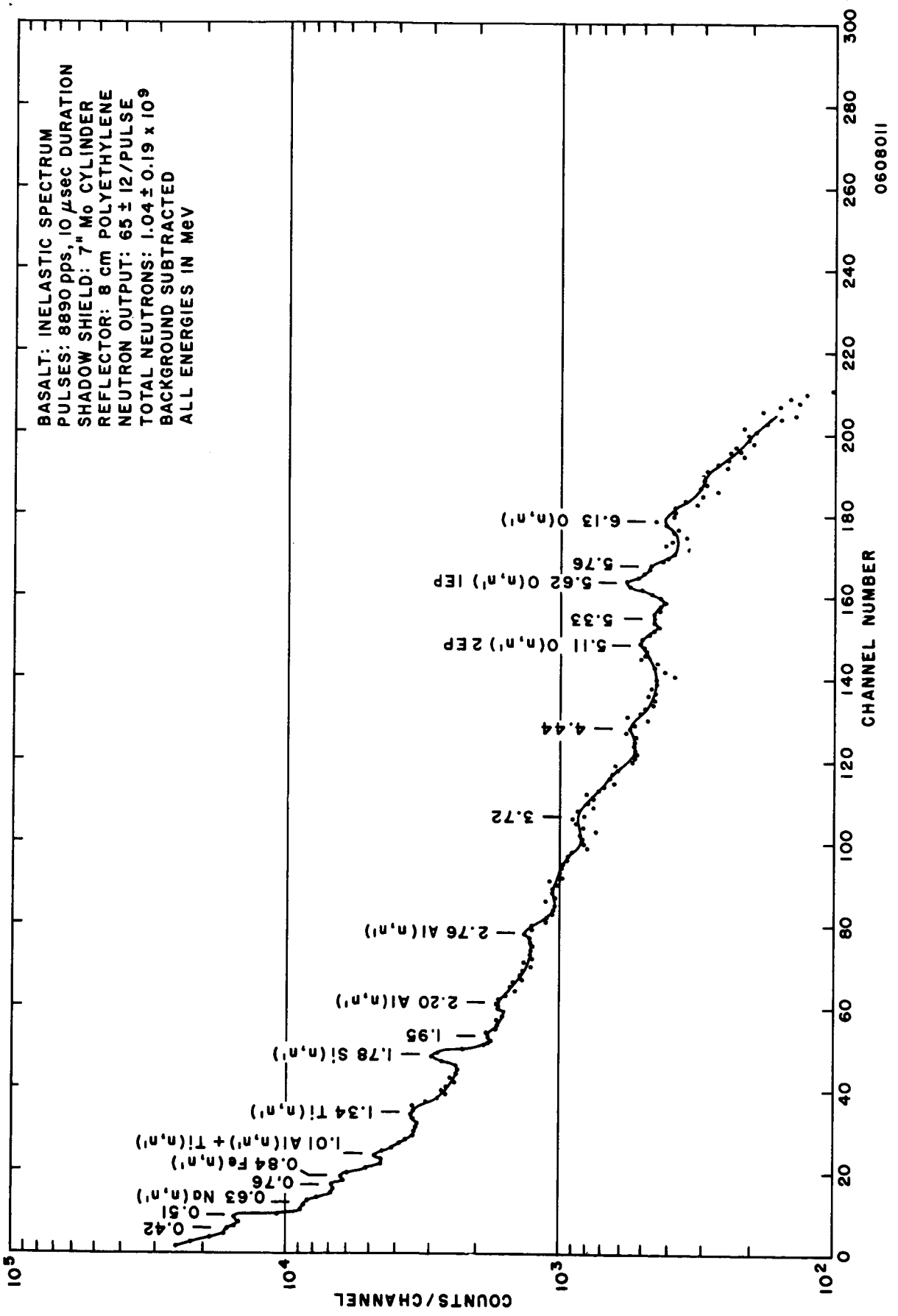

Figure 13 INELASTIC SPECTRUM OF BASALT (8-cm-thick Polyethylene Reflector, 7 in. Mo Shadow Shield)

Since the capture gamma-ray spectrum from basalt exhibits rather intense high-energy peaks (e.g., peaks from iron, titanium, and calcium), further experiments will be necessary to determine how the reflector thickness affects the capture gamma-ray spectra from granite (which contains less iron, titanium, and calcium) and from dunite (which contains less titanium and calcium but more magnesium). These experiments will have to be performed before a final decision can be made regarding the neutron reflector thickness to be used in the probe. However, it is expected that the final thickness will be between 4 and 8 cm.

In order to determine what effect the reflector has on the inelastic spectrum from basalt, inelastic spectra were obtained without a reflector using the 6-in.-truncated conical copper shadow shield (Figure 14) and the 7-in.-cylindrical copper shadow shield (Figure 15). These spectra were obtained under the same conditions as those of Figures 11 and 12 except for small differences in the neutron outputs. Comparisons of Figures 11 and 14 and of Figures 12 and 15 indicate that the use of an 8-cm-thick polyethylene reflector does not affect the inelastic spectrum.

Magnetic and Electrostatic Shielding

It was found that the voltage multiplier in the SANDIA neutron generator produces electromagnetic interference which degrades the spectral data. Shielding of the generator, the crystal preamplifier, and the photomultiplier tube with electromagnetic shielding material was found to eliminate this interference. It was decided that, in the probe, the photomultiplier tube, the preamplifier, and the neutron generator would all have to be shielded with electromagnetic shielding material.

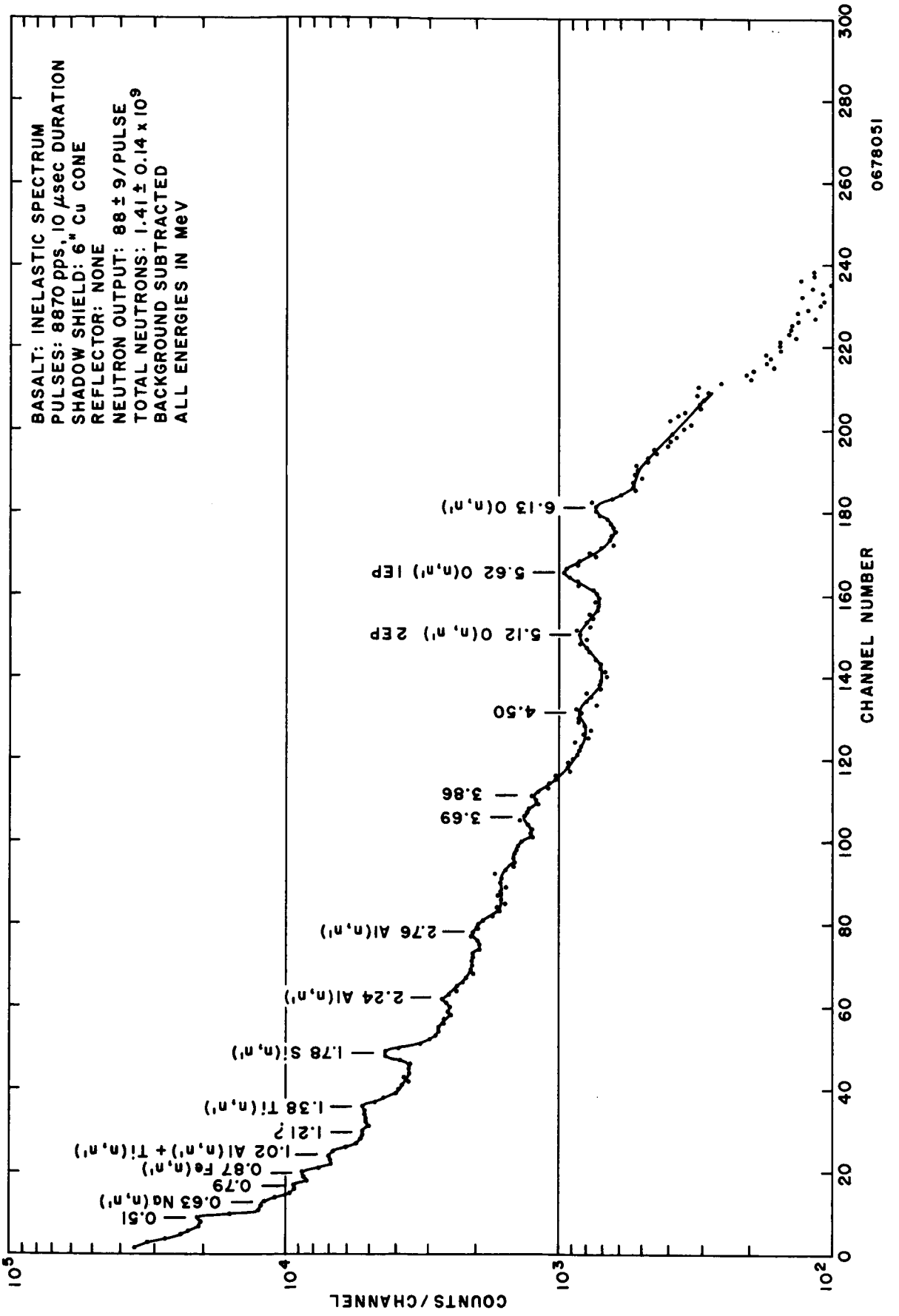

Figure 14 INELASTIC SPECTRUM OF BASALT (No Reflector, 6 in. Cu Shadow Shield)

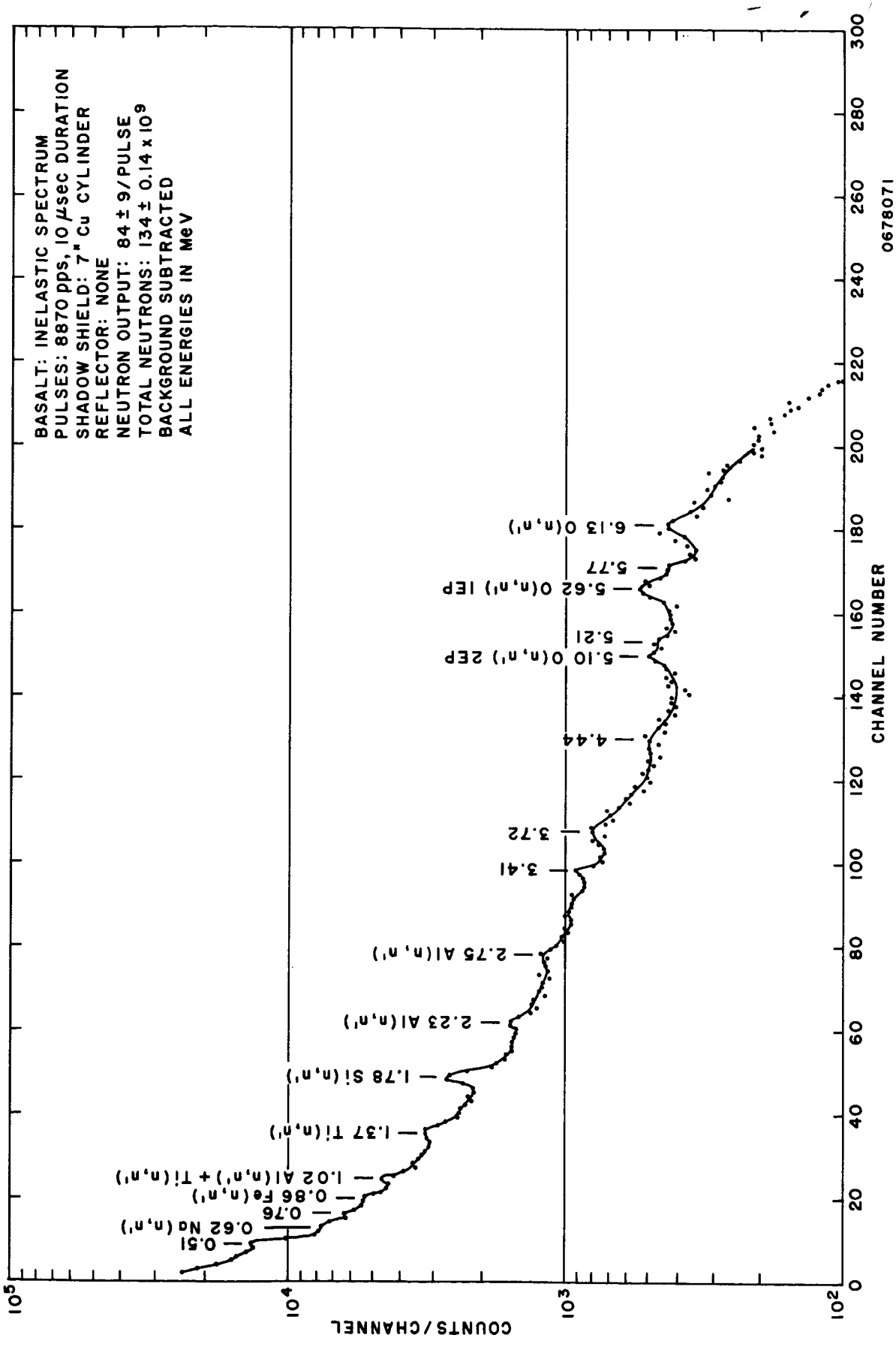

Figure 15 INELASTIC SPECTRUM OF BASALT (No Reflector, 7 in. Cu Shadow Shield)

General Probe Configuration

Since the thickness of the hydrogenous neutron reflector material to be used is still uncertain, the basic geometry of the probe was designed to accommodate both a 4-cm- and an 8-cm-thick polyethylene reflector. A general view of the probe with no reflector is shown in Figure 16. A view with the 8-cm-reflector in place is shown in Figure 17.

The direct shield interposes 6.5 in. of molybdenum between the neutron source and the crystal. This provides the same total neutron removal cross section as 6 in. of copper. A cylindrical shape is used for the back 4.5-in. portion of the direct shield to absorb the hydrogen capture gamma rays produced in the lucite and oil contained in the neutron generator. For 2-MeV gammas, the transmission of 4.5 in. of molybdenum is less than 1 percent or about the same as that of 3.25 in. of lead.

The centerline of the probe is 2 5/8 in. from the sample surface. This dimension is determined by the overall size of the shielded NaI crystal which rests almost on the sample surface. The distance from the neutron source to the center of the crystal is 11 1/4 in.

Estimates for the weight of the various components are tabulated in Table 2 for each of the three probe configurations. The estimated total weight varies from 50 to 92 pounds, depending on the reflector thickness.

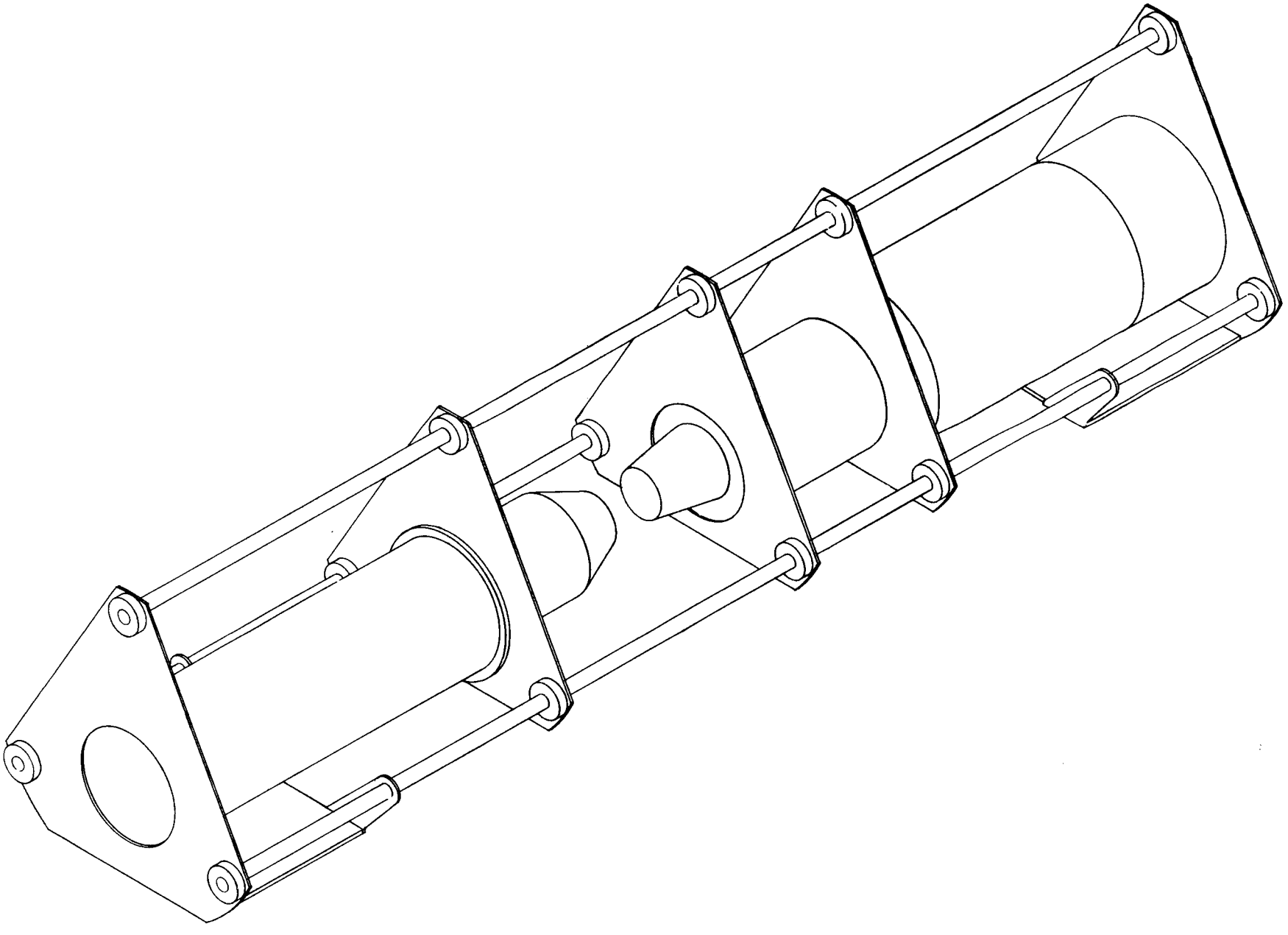

Figure 16 COMBINED NEUTRON EXPERIMENT DETECTOR PROBE (View with no Reflector)

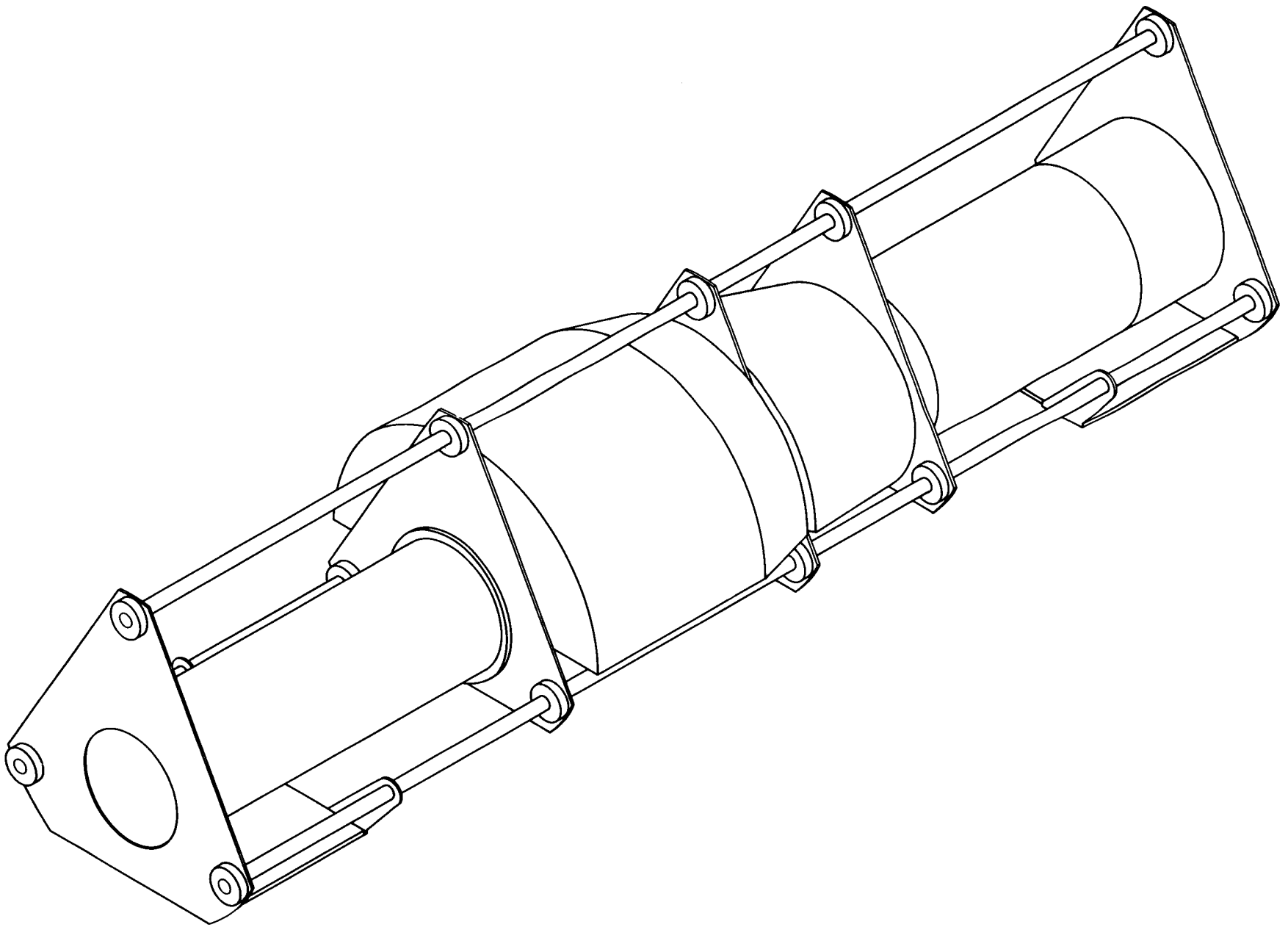

Figure 17 COMBINED NEUTRON EXPERIMENT DETECTOR PROBE (View with 8-cm-thick Reflector)

Table 2. WEIGHT ESTIMATES FOR THREE DIFFERENT PROBE CONFIGURATIONS

Component	No Reflector (lb)	With 4-cm-Reflector (lb)	With 8-cm-Reflector (lb)
Generator	7.5	7.5	7.5
Direct Shield	17.5	17.5	17.5
Crystal Assembly	4.0	4.0	4.0
Li Can	1.0	1.0	1.0
Reflector	0.0	3.1	7.5
Reflector Shield	0.0	12.0	34.2
Miscellaneous	20.0	20.0	20.0
	50.0	65.1	91.7

III. SUMMARY AND CONCLUSIONS

During this reporting period the design of the detector probe was completed. Since experimental results indicated that the measurement of hydrogen can be accomplished if the crystal is shielded from the gamma rays produced in the neutron reflector, the shape of the shadow shield was designed to shield the crystal from fast neutrons and from gamma rays originating in the reflector and in the neutron generator. Also, since the experimental results obtained by taking the capture gamma-ray spectrum of basalt for varying neutron reflector thicknesses were inconclusive, the basic geometry of the probe was designed to accommodate both a 4-cm- and an 8-cm-thick neutron reflector. Further experiments will be undertaken during the next reporting period to establish the necessary neutron reflector thickness.

A sample of crushed olivine is presently being obtained from the Northwest Olivine Company, Seattle, Washington. Capture gamma-ray and cyclic activation analyses will be performed on this sample during the next reporting period.

In addition, the probe will be fabricated and will be used to obtain capture gamma-ray, inelastic, and cyclic activation spectra of the various samples (basalt, granite, and dunite).

APPENDIX A

NEUTRON MONITORING

Previously (see Report No. IITRI-A6155-5), the 14-MeV neutron output of the Van de Graaff generator was monitored by a BF_3 counter positioned under the large sample container. Neutron output measurements were performed using copper activation foils to obtain the 14-MeV neutron output per BF_3 count, enabling a BF_3 count rate to be related directly to 14-MeV neutron output. This indirect method of monitoring the 14-MeV neutron output had the disadvantages that, for a given 14-MeV neutron output, the BF_3 count rate was sensitive to the sample material and to the amount of reflector material used.

Because of the disadvantages of the BF_3 monitor, a neutron monitoring system employing a plastic scintillator and a Teflon sample* placed near the target (neutron source) was devised. The plastic scintillator output passes through a discriminator which is set (using a Pu-Be neutron source) to pass only counts from neutrons whose energies are greater than about 9 MeV. The F^{18} activity in the Teflon produced by the F^{19} $(n,2n)F^{18}$ reaction (Q = -10.4 MeV) is gross-counted after a run by a well-crystal. Both the plastic scintillator and the Teflon were calibrated using copper activation foils so that a scintillator count rate and a Teflon count rate can be related directly to 14-MeV neutron output. Since these two methods are sensitive only to high-energy neutrons, they are independent of sample material and reflector thickness.

The plastic scintillator is also being used during the setup of the capture gamma-ray runs to monitor the neutrons produced between pulses. This is done to ensure that the neutron generator is pulsing correctly and not producing appreciable dark current (neutronsbetween pulses).

---

*Suggested by W. R. Mills, Mobil Oil Corporation.